Journal of Materials Chemistry C

Accepted Manuscript

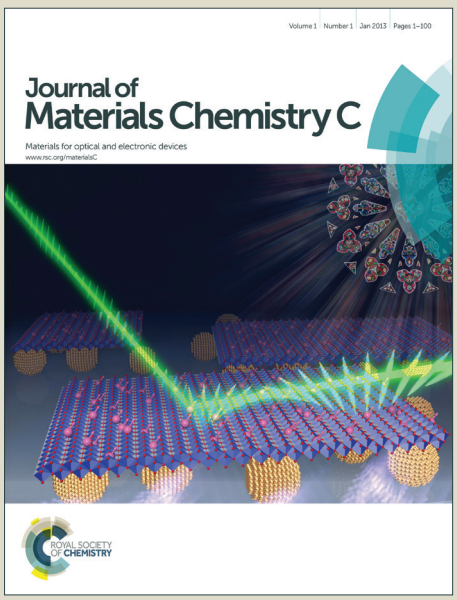

ROYAL SOCIETY OF CHEMISTRY

www.rsc.org/materialsC

Journal of Materials Chemistry RSCPublishing

ARTICLE

Hydrogenation of silicene with tensile strains

Cite this: DOI: 10.1039/x0xx00000x

W. C. Wu,[a] Z. M. Ao,[b*] C. H. Yang,[c] S. Li,[d] G. X. Wang,[b] C. M. Li,[e] and S. Li[a]

Received xxxxxxx,
Accepted xxxxxxx

DOI: 10.1039/x0xx00000x

www.rsc.org/

Hydrogenation of silicene has been shown to be an efficient way to open the band gap of silicene and manipulate its electronic properties for application in electronic devices. However, the reaction energy barrier of silicene hydrogenation is quite high, which prevents the occurrence of this chemical reaction. Using density functional theory calculations, we propose an alternative approach to reduce the energy barrier, thus facilitating hydrogenation of silicene. Our results demonstrate that biaxial strain and uniaxial tensile strains along armchair direction can reduce the energy barrier of H_2 dissociative adsorption on silicene significantly, and the barrier decreases as the strains increase. However, the biaxial strain has better effect on the energy barrier reduction. It is found that the barrier reduces from 1.71 to 0.24 eV when the biaxial strain reaches the critical value of about 12%, above which the structure of silicene after hydrogenation would be destroyed. In this way, the reaction time for the hydrogenation of silicene can be reduced significantly from 8.06×10^{16} to 1.68×10^{-8} s. The mechanism of the effect of tensile strains can be understood through analysing density of states of the system and atomic charge transfer during hydrogenation.

Introduction

Silicene, a two-dimensional honeycomb network of silicon atoms, has attracted lots of interests since it was firstly predicted in 1994.[1-10] Though silicene is the silicon analogue of graphene, silicene has been confirmed to be energetically favourable to be a low buckled honeycomb structure, because in silicon the sp^3 hybridization is more stable than the sp^2 hybridization, which is converse to graphene.[11] By investigating the band structure of this buckled structure, it is found that alike graphene, there are linear dispersions at the Dirac points K and K' of the hexagonal Brillouin zone, indicating the semimetallic or zero band gap semiconducting character of silicene.[12-15] This structure has been confirmed by density functional theory (DFT) studies[16] and phonon dispersion calculations.[17] Several other works have also confirmed that silicene is a zero band gap semiconductor.[18-20] Recently, the single layer sheet of silicene has been obtained via chemical exfoliation[21] and also successfully fabricated on Ag substrates.[22-25] As silicon has similar chemical properties with carbon, and properties of graphene can been controlled by hybridising,[26-28] external electric field,[29,30] doping,[31,32] chirality[33] and strain,[34,35] it is desirable to manipulate the properties of silicene for its future potential applications.

With these expectations and methods, various breakthroughs on silicene have been reported. For example, it is found that the band gaps of silicene adsorbed with F, Cl, Br and I have a nonmonotonic change as the periodic number of the halogen elements increases.[20] Through functionalization of silicene, particularly hydrogenation, it is found that the properties of silicene can be tuned by the hydrogenation ratio. For example, half hydrogenated freestanding silicene generates an indirect band gap (about 0.84 eV) and becomes a ferromagnetic semiconductor based on generalized gradient approximation (GGA) calculation.[16] Similar magnetic transition is also found in the hydrogenation of silicene on a substrate.[36] Furthermore, in the fully hydrogenated silicene (silicane), a 2 eV indirect band gap is found, leading the silicane to be an insulator based on local density approximation (LDA) calculation.[37] Therefore, by applying a proper hydrogenation ratio, band structure of silicene is tuneable, which could transfer the system to be metallic, semiconducting or insulating.[16,19,38]

However, according to the study of binding energy on low buckled silicene based on DFT-GGA calculations,[39] the energy barrier of hydrogen atom adsorption in silicene is too high compared to that of gaseous hydrogen molecules. This indicates that the dissociative adsorption of hydrogen on silicene would be difficult due to the passive surface of silicene. The dissociation possibility can be understood by the energy barrier, which is defined as the energy difference between the reactant and the highest energy state along the minimum energy reaction paths (transition state TS). With high energy barrier, reactions could not go effectively or not even happen.[40,41] Recently, it was reported that strain can significantly modify the atomic structures, binding energies, mechanical and electronic properties of pure and hydrogenated graphene.[42-45] For the hydrogenation of graphene, the tensile strain has been found to effectively lower the out-plane diffusion of H atoms, which makes the diffusion possible at room temperature.[42] Furthermore, by applying strain to the graphene, the barrier of the dissociation of molecular hydrogen greatly decreases and the process of the hydrogenation changes from endothermic to exothermic.[43] In addition, silicene can also be converted to semimetal by a tensile strain of 7% and turned into a conventional metal under larger homogeneous strain.[44] Therefore, strain is expected to be an effective way to manipulate the electronic properties and the energy barrier for hydrogenation of silicene.

In this work, in order to reduce the energy barrier of silicene

hydrogenation, biaxial strain and uniaxial tensile strains along both zigzag and armchair directions are applied and the corresponding effects on hydrogenation are investigated through DFT calculations. The hydrogenation of silicene can be understood through the calculation of the reaction pathway under the strains. The mechanism of the energy barrier reduction induced by the tensile strains can be analysed through partial density of states (PDOS) and atomic charge transfer between H_2 and silicene. In addition, the effect of hydrogenation on the electronic properties of silicene with strains is also discussed.

Simulation methodology

The spin-polarised DFT calculations were performed using the DMol[3] module in Materials Studio package. LDA with the Perdew and Wang functional is employed as the exchange-correlation functional. To consider the effect of van der Waals interface, OBS method for DFT-D correction is used. A double numerical plus polarization (DNP) was used as the basis set. The convergence tolerance of energy is taken as 10^{-5} Ha (1 Ha = 27.21 eV), with a maximum allowed force and displacement of 0.002 Ha and 0.005 Å respectively. Linear synchronous transition/quadratic synchronous transit (LST/QST)[1] and nudged elastic band (NEB)[46] tools in DMol[3] were also employed to investigate the minimum energy pathway for hydrogen dissociative adsorption on silicene. Three-dimensional periodic boundary conditions are taken in the simulation. A 4×4×1 supercell is adopted for all the calculations with a vacuum width of 18 Å above the layer to minimize the interlayer interaction as presented in Fig. 1. The calculations were performed with 6×6×1 K-point set, and all atoms were relaxed to their most stable geometry. To apply biaxial or uniaxial tensile strains to silicene, the lattice parameter of both *b* and *c* or only *b* or *c* is increased at different ratio, as indicated by the arrows in Fig. 1. Note that when we did the structure relaxation under a uniaxial tensile, the lattices along the direction of the applied tension strain and the direction normal to the silicene are fixed, while the lattice of the other direction is allowed to relax. For example along the zigzag direction as shown in Fig. 1(c), the lattice constants along *c* and the direction normal to the silicene surface are fixed, while the lattice constant along *b* is allowed to relax.

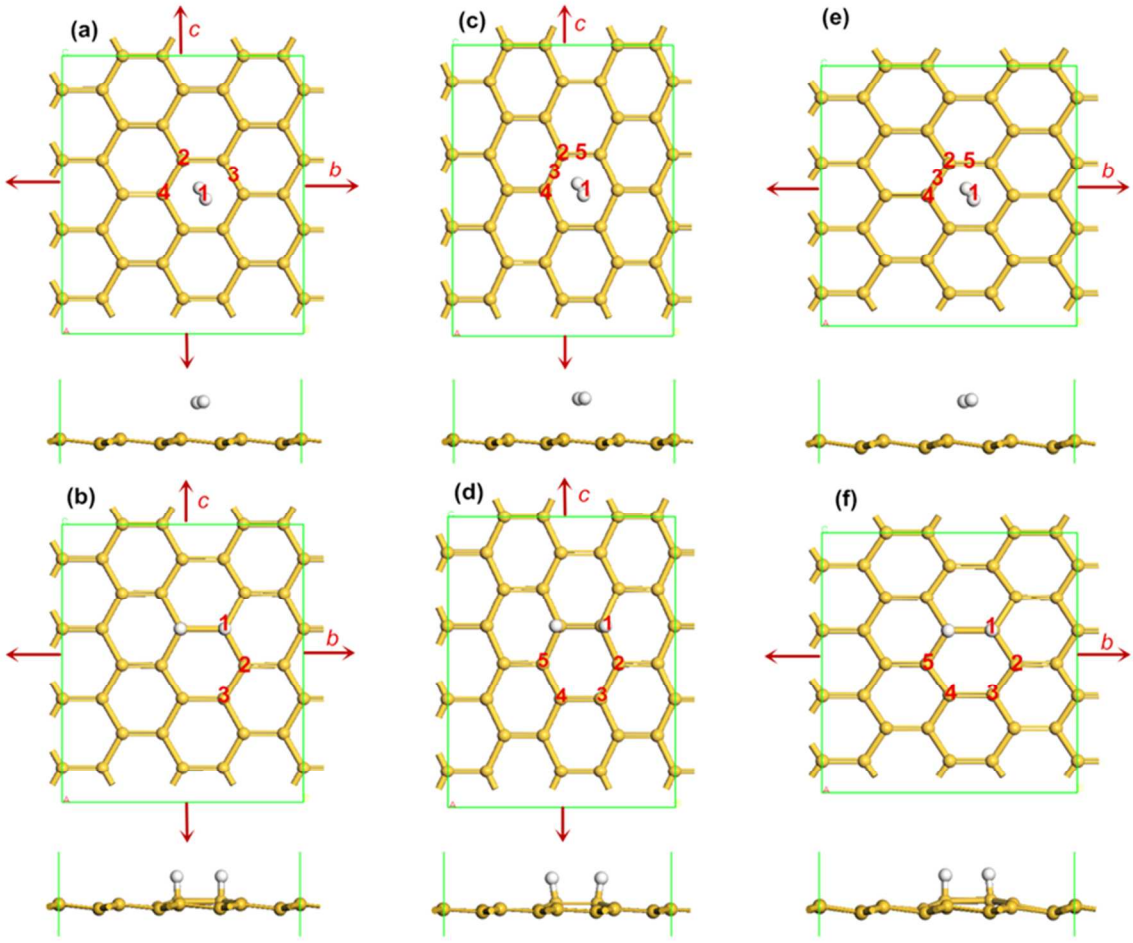

Fig. 1 The initial and final structures of a H_2 molecule on silicene before and after dissociative adsorption with biaxial strain [(a) and (b)], uniaxial strain along zigzag[(c) and (d)] and along armchair [(e) and (f)] directions. The possible positions for an H_2 molecule physically adsorbed in silicene or the possible positions of the second H atom when 2 H atoms chemically adsorbed on silicene are indicated by numbers. The direction of the tensile strain is denoted by arrows. The numbers in the top panel of the figure denote the different possible adsorption position of the H_2 molecule, while the numbers in the bottom panel of the figure denote the different possible bonding position of the second H atom.

Table 1. The total energy, adsorption energy, and the distance between the H_2 molecule and the silicene layer $D_{H\text{-}Si}$ in all the possible structures before hydrogenation under different biaxial tensile strain. For total energy, it is relative energy to that of H_2 adsorption at position 1 of silicene without strain.

	Total energy(eV)				Adsorption energy(eV)				$D_{H\text{-}Si}$(Å)			
Strain	1	2	3	4	1	2	3	4	1	2	3	4
0	0	0.09	0.08	0.08	-0.29	-0.20	-0.21	-0.21	2.49	3.04	3.06	2.98
5%	3.18	3.29	3.28	3.28	-0.30	-0.19	-0.20	-0.20	2.44	3.22	3.25	3.11
10%	10.86	10.96	10.94	10.96	-0.28	-0.18	-0.20	-0.18	2.34	3.18	3.10	3.10
12%	14.15	14.26	14.24	14.25	-0.55	-0.44	-0.46	-0.45	2.31	3.26	3.13	3.12

Table 2 The total energy, adsorption energy, and the distance between the H_2 molecule and the silicene layer $D_{H\text{-}Si}$ in the five possible structures before hydrogenation under different uniaxial tensile strain along zigzag direction. For total energy, it is relative energy to that of H_2 adsorption at the position 1 of silicene without strain.

	Total energy(eV)					Adsorption energy(eV)					$D_{H\text{-}Si}$(Å)				
Strain	1	2	3	4	5	1	2	3	4	5	1	2	3	4	5
0	0	0.09	0.08	0.08	0.08	-0.29	-0.20	-0.21	-0.21	-0.21	2.49	3.04	3.06	2.98	3.03
5%	1.72	1.80	1.84	1.80	1.80	-0.28	-0.20	-0.19	-0.20	-0.20	2.52	3.19	3.15	3.08	3.18
10%	4.35	4.45	4.44	4.45	4.45	-0.28	-0.18	-0.19	-0.19	-0.19	2.46	3.19	3.19	3.08	3.18
14%	7.57	7.66	7.64	7.64	7.64	-0.27	-0.18	-0.20	-0.20	-0.19	2.53	3.26	3.24	3.19	3.22

Table 3 The total energy, adsorption energy, and the distance between the H_2 molecule and the silicene layer $D_{H\text{-}Si}$ in the five possible structures before hydrogenation under different uniaxial tensile strain along armchair direction. For total energy, it is relative energy to that of H_2 adsorption at the position 1 of silicene without strain.

	Total energy(eV)					Adsorption energy(eV)					$D_{H\text{-}Si}$(Å)				
Strain	1	2	3	4	5	1	2	3	4	5	1	2	3	4	5
0	0	0.09	0.08	0.08	0.08	-0.29	-0.20	-0.21	-0.21	-0.21	2.49	3.04	3.06	2.98	3.03
5%	1.32	1.42	1.41	1.41	1.40	-0.29	-0.19	-0.20	-0.20	-0.20	2.52	3.14	3.13	3.08	3.08
10%	4.63	4.73	4.72	4.73	4.72	-0.29	-0.19	-0.19	-0.19	-0.20	2.40	3.23	3.19	3.12	3.14
13%	7.33	7.43	7.42	7.42	7.41	-0.29	-0.18	-0.19	-0.19	-0.20	2.36	3.32	3.18	3.15	3.15

For the adsorption of one H_2 molecule on silicene, the adsorption energy E_{ad} is defined as,

$$E_{ad}=E_{H2+silicene}-(E_{silicene}+E_{H2}) \quad (1a)$$

where $E_{H2+silicene}$, $E_{silicene}$, and E_{H2} denote the total energies of silicene with a H_2 molecules adsorbed, bare silicene, and a H_2 molecule respectively. After hydrogenation, the binding energy of H atoms on silicene $E_{Si\text{-}H}$ can be determined as,

$$E_{Si\text{-}H}=E_{2H+silicene}-(E_{silicene}+2E_{H}) \quad (1b)$$

where subscripts 2H+silicene and H denote the silicene with 2 H atoms chemically adsorbed and a free H atom respectively.

Results and discussion

Before hydrogenation, the H_2 molecule is weakly physically adsorbed on silicene. Under the biaxial tensile strain, silicene expends symmetrically, there are 4 possible adsorption positions for the H_2 molecule as indicated in Fig. 1(a): positions 2 and 4 on the top of a silicon atom in the higher or lower plane of the buckled structure, position 3 over the middle of a Si-Si bond and position 1 at the center of a Si ring. In order to determine the most stable structure, we calculate all the four possible positions under different strains. Note that the strain limit for hydrogenated silicene is 12% under biaxial strain, 14% under uniaxial strain along zigzag direction and 13% under uniaxial strain along armchair direction, if further increasing the strain, the Si-Si bond of the two silicon atoms which are bonded with the hydrogen atoms or other Si-Si bonds would break, which should be avoided in applications. The result also agrees with the reported result that the structure of buckled silicene is stable when the tensile strain is smaller than 14%.[47] Other works also confirm the stability of silicene under similar strains.[48] From phonon dispersions calculations,[49,50] it is also known that silicene is stable under strains when the strain is smaller than 14%. The results in Table 1 show that under different biaxial tensile strain the total energy and adsorption energy of a H_2 molecule on silicene at position 2-4 are almost the same but those at position 1 are much lower, especially for the adsorption energy. Thus, the H_2 molecule is favourable to adsorb at the hollow site of the Si ring regardless the intensity of the strain, which is easy to understand because the silicene expends in symmetry under the biaxial tensile strain. This configuration is considered to be the reactant for the silicene hydrogenation reaction. Note that the distance between the H_2 molecule and the silicene layer $D_{H\text{-}Si}$ at position 1 is always shorter than that in the other three positions at a given strain due to the stronger adsorption energy.

Silicene under uniaxial strains along both zigzag and armchair directions is studied in a similar way as shown in Figs. 1(c) and 1(e), respectively. Since the structure of silicene is not symmetric any more due to the lattice deformation under an uniaxial strain, there are more possible positions for the hydrogen molecule adsorption, such as on the top of a silicon atom either on up (position 2) or bottom layer (position 4), on the top of a Si-Si bond (there are two types of Si-Si bonds due to the deformation, thus two possible positions: positions 3 and 5) and at the hollow site of a Si ring (position 1). The results of system total energy, adsorption energy of a H_2 molecule on silicene under different uniaxial tensile strains along zigzag and armchair directions are shown in Table 2 and Table 3, respectively.

Table 4 The total energy and binding energy of all the possible structures after hydrogenation under biaxial tensile strain. The energy barrier and reaction energy to final structures 1 and 3 are also listed. For total energy, it is relative energy to that of the structure with the second H atom adsorption at the position 1 of silicene without strain.

	Total energy(eV)			Binding energy(eV)			Energy barrier(eV)	Reaction Energy(eV)
Strain	1	2	3	1	2	3	1	1
0	0	0.55	0.12	-5.50	-4.94	-5.37	1.71	-0.21
5%	3.04	3.63	3.12	-5.65	-5.06	-5.57	1.49	-0.35
10%	10.20	10.55	10.34	-6.15	-5.80	-6.00	1.06	-0.74
12%	13.44	13.66	13.50	-6.46	-6.24	-6.40	0.24	-0.85

Table 5 The total energy and binding energy of all the possible structures after hydrogenation under uniaxial tensile strain along zigzag direction. The energy barrier and reaction energy to final structures 1, 3 and 5 are also listed. For total energy, it is relative energy to that of the structure with the second H atom adsorption at the position 1 of silicene without strain.

	Total energy(eV)					Binding energy(eV)					Energy barrier (eV)			Reaction Energy (eV)		
Strain	1	2	3	4	5	1	2	3	4	5	1	3	5	1	3	5
0	0	0.55	0.12	0.57	0.19	-5.50	-4.94	-5.38	-4.92	-5.31	1.71	1.82	1.98	-0.21	-0.06	-0.24
5%	1.59	1.15	1.56	1.16	1.51	-5.62	5.18	-5.59	-5.19	-5.55	1.55	1.66	1.66	-0.29	-0.17	-0.32
10%	4.07	4.49	4.15	4.51	4.02	-5.78	-5.35	-5.70	-5.34	-5.82	1.40	1.41	1.48	-0.48	-0.36	-0.46
14%	6.61	7.25	7.02	7.22	7.02	-6.44	-5.80	-6.02	-5.83	-6.03	1.26	1.38	1.35	-0.70	-0.57	-0.60

Table 6 The total energy and binding energy of all the possible structures after hydrogenation under uniaxial tensile strain along armchair direction. The energy barrier and reaction energy to final structures 1, 3 and 5 are also listed. For total energy, it is relative energy to that of the structure with the second H atom adsorption at the position 1 of silicene without strain.

	Total energy(eV)					Binding energy(eV)					Energy barrier (eV)			Reaction Energy (eV)		
Strain	1	2	3	4	5	1	2	3	4	5	1	3	5	1	3	5
0	0	0.55	0.12	0.57	0.19	-5.50	-4.94	-5.38	-4.92	-5.31	1.71	1.82	1.98	-0.21	-0.06	-0.24
5%	1.20	1.84	1.38	1.83	1.30	-5.52	-4.97	-5.43	-4.98	-5.62	1.64	1.73	1.86	-0.22	-0.11	-0.28
10%	4.46	5.04	4.53	5.04	4.36	-5.66	-5.08	-5.59	-5.08	-5.76	1.38	1.52	1.67	-0.36	-0.28	-0.33
13%	7.01	7.60	7.10	7.43	6.93	-5.81	-5.23	-5.72	-5.38	-5.88	0.26	0.96	1.31	-0.49	0.40	-0.43

It is shown that the structure with the hydrogen molecule at the hallow site (position1) of a Si ring is the most stable structure that has the lowest total energy, shortest $D_{H\text{-}Si}$ and the strongest binding energy under any strain. Although the symmetry of silicene is destroyed under uniaxial strain, the H_2 molecule still prefers to adsorb at the hollow site of a Si ring (position 1) regardless the intensity of strain, which is similar to the result of the case under biaxial strain. In the subsequent hydrogen dissociative adsorption, the possible positions under biaxial tensile strains for the two adsorbed hydrogen atoms are shown in Fig. 1(b). All the possible configurations are calculated and the corresponding results are listed in Table 4. It is found that under biaxial tensile strain as shown in Fig. 1(b), the two H atoms binds with Si atoms in the form of covalent bond, and there are three possible configurations. The structure with the ortho position of the two hydrogen atoms, *i.e.* the second H atom at position 1, has much lower energy and stronger binding energy under any strain. Therefore, this possible reaction pathways for hydrogen dissociative adsorption on silicene, *i.e.* from the reactant structure with a H_2 molecule physically adsorbed at position 1 to the product structure with the second H atoms binding at position 1, is calculated. Figure 2 shows the minimum reaction pathway of a H_2 molecule dissociative adsorption on silicene without strain for an example for how to determine the dissociative energy barrier and obtain other relevant information. The structures as shown in Figs. 1(a) and 1(b) are reactant and product, respectively. After LST/QST and NBE calculations, the energy minimum dissociative absorption pathway is shown in Fig. 2. From this figure, the reaction energy barrier $E_{bar} = E_{TS} - E_{IS}$ is 1.71 eV. Note that before TS, the H_2 molecule adjusts its position over silicene then the H_2 molecule is dissociated into two free H atoms with one of the H atoms binding with a Si atom nearby at the top layer while the other H atom keeps free, as shown as the TS in Fig. 2. In addition, the Si atom that is going to bind with the free H atom has also shifted upwards, but the two H atoms are still closed to each other with strong interaction, which prevents the binding between the free H atom and the Si atom. At the final state FS, the distance of the two H atoms increases, and thus the other free H atom also binds with the nearest Si atom as shown in Fig. 2. Therefore, this reaction can be separated into two steps: the H_2 molecule is first dissociated into two H atoms, and then one of them binds with a Si atom nearby while the other one is free; at the second step, the two H atoms adjust their position and the other H atom also binds with its nearest Si atom. Although this reaction releases energy about 0.21 eV in total (E_{FS} - E_{IS}), there is a high potential energy barrier of 1.71 eV for the first step. Consequently, the first step becomes a rate-limiting step because of a large energy needed.

It is reported that a reaction is difficult to happen at room temperature if the reaction energy barrier is higher than 0.75 eV.[46] Due to the high energy barrier of 1.71 eV for this hydrogenation process, it is considered to be difficult for the reaction to go through at room temperature, high reaction temperature or other external energy source is required. Therefore, it is desirable to reduce the hydrogenation energy barrier. Applying tensile strain is an alternative way to alter the electronic distribution of silicene,[47] thus changing its chemical potential. As mentioned before, it has been proved that strain can modify the atomic structures and the electronic properties of silicene.[47] In addition, the barrier of the dissociation of molecular hydrogen on graphene has been greatly reduced by

applying strain to graphene,[43] which is the current challenge for the hydrogenation of silicene. Therefore, tensile strain is considered here to investigate the possibility of reducing the hydrogenation energy barrier of silicene.

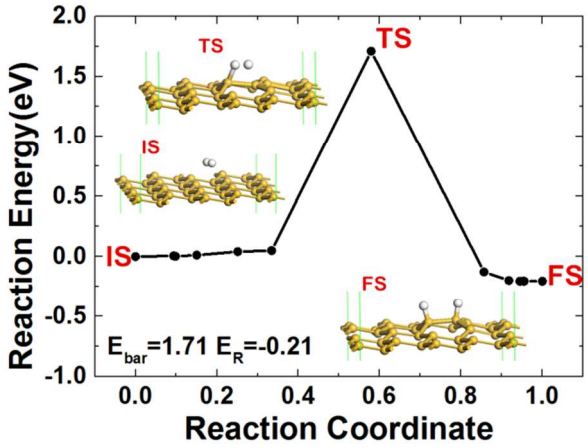

Fig. 2 The reaction pathway of the dissociative adsorption of a H_2 molecule on silicene without strain from the structure as shown in Fig. 1(a) to the structure as shown in Fig. 1(b). The energy of reactant IS is taken to be zero. IS, TS and FS denote initial structure, transition structure, and final structure, respectively. E_{bar} is the energy barrier, E_R is the reaction energy, and their unit is eV.

Using the same method, the hydrogen dissociative adsorption on silicene under different biaxial tensile strain is calculated. The structure with the second H atom at position 1 as the product is considered, and the results are listed in Table 4. It is clearly shown that the energy barrier reduced when a biaxial tensile strain is present. The barrier decreases as the strain increases. When reaching the maximum possible strain of 12%, the barrier is minimum of 0.24 eV. Under uniaxial strains, there are five possible configurations for the product as shown in Figs. 1(d) and 1(f) where 5 possible binding positions for the second H atom are indicated. After geometry optimization, the results are shown in Tables 5 and 6, respectively. Similar to the case of biaxial strain, it is found that the hydrogenated silicene with two hydrogen atoms in structures 1, 3 and 5 in Figs. 1(d) and 1(f) have similar and lower total energy with stronger binding energy under the both two types of uniaxial strains, indicating all the three positions being possible after the H_2 molecule dissociative adsorption. Therefore, all the three reaction pathways from the structure in Fig. 1(c) to the structure in Fig. 1(d) with the second H atom at position 1, 3 and 5, and the three reaction pathways from Fig. 1(e) to the structure in Fig. 1(f) with the second H atom at position 1, 3 and 5 are considered. The results of corresponding reaction energy barrier and reaction energy are listed in Tables 5 and 6, respectively. It is found that the energy barrier is always the lowest the reaction to the position 1 under different uniaxial strains, which indicates that this reaction is preferred. Therefore, the pathway of hydrogen dissociative adsorption on silicene under these two types of uniaxial tensile strains from the initial structure with the H_2 molecule adsorbed on the hallow site of a Si ring to the final structure with the second H atom at position 1 is calculated and discussed in the following.

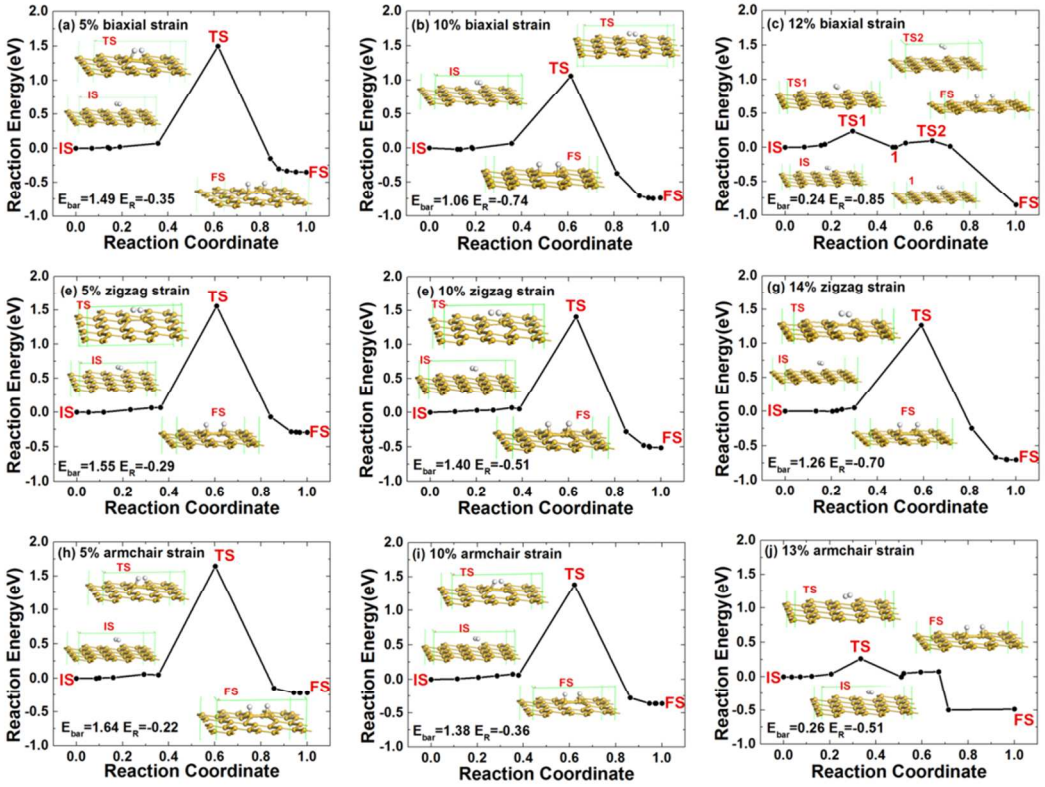

Fig. 3 The pathway of dissociative adsorption of a H_2 molecule on silicene with increasing biaxial tensile strain [(a)-(c)], uniaxial tensile strain along zigzag direction [(d)-(f)] and along armchair direction [(h)-(j)].Transition structure and energy minimum states 1 are represented by TS and 1 respectively. The energy of IS is set to be zero. The E_{bar} and E_R are energy barrier and reaction energy respectively and their units are eV.

To better understand the effect of the tensile strain, the hydrogenation pathways of silicene under different strain are shown in Fig. 3. Figs. 3(a)-(c) represent the pathways under the biaxial tensile strain along the energy minimum pathway to structure 1 in Fig. 1(b). Figs. 3(e)-(g) are for the cases under zigzag direction uniaxial tensile strain along the energy minimum pathway to structure 1 in Fig. 1(d) and Figs. 3(h)-(j) demonstrate the pathways under armchair direction uniaxial tensile strain along the energy minimum pathway to structure 1. As shown in the figure, the configurations before and after hydrogenation reconstruct as expected under strains. At transition state (TS), the H_2 molecule is dissociated into two separate H atoms at TS (except in Figs. 3(c) and 3(j) with molecular H_2). There are not covalent bonds yet between the two H atoms and silicene, except in Figs. 3(a), 3(h) and 3(i), where one of the H atoms binds with a Si atom in the upper layer of silicene similar to the case without strain in Fig. 2. This could be understood by analysing the bond length change of Si-Si and H-H bonds. It is known that the length of Si-Si bond in silicene increases as the strain increasing. Under the strain of 10%, the Si-Si bond becomes weak enough to allow the formation of Si-H bond over the silicene layer. On the other side, when the binding of Si-Si bonds in silicene becomes weaker under the strain, the interaction between the H atoms become stronger, which is indicated by the shorter distance between the two H atoms $D_{H\text{-}H}$. It is found that $D_{H\text{-}H}$ decreases when strain increases. This is also consistent with the general rule that the interaction in a molecule is stronger when the binding in a substrate becomes weaker.[29,48] The stronger H-H interaction prevents the covalent bond formation between H and Si atoms under the limit strain although the Si-Si bond is weak enough at this case. On the other hand, although the Si-Si bond is still strong in the case without strain, the H-H bond is the weakest, which can also induce the formation of Si-H bond at transition state as shown in Fig. 2. Therefore, the Si-H bond at transition state forms only when a balance is achieved between the interactions of Si-Si and H-H bonds. After transition state, the distance between the two H atoms increases and the corresponding interaction decreases gradually, then the two H atoms bind with the corresponding Si atoms as shown as FS in Fig. 3.

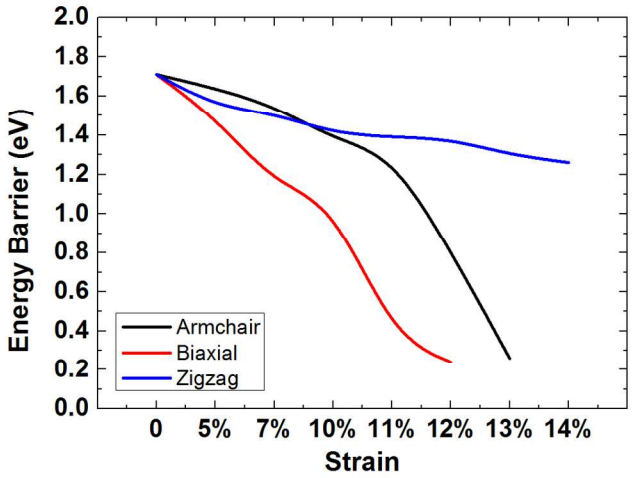

Fig. 4 Energy barrier of the dissociative adsorption of a H_2 molecule on silicene under increasing tensile strain. The black, red and blue lines stand for the results under biaxial tensile strain, uniaxial tensile strain along armchair and zigzag directions.

The corresponding energy barrier and reaction energy for a H_2 molecule dissociative adsorption on silicene under different strains are also shown in Fig. 3. It is found that the energy barrier decreases with the strains increase for all three types of strain, while the corresponding reaction energy becomes more negative. Therefore, the H_2 molecule is easier to be dissociated under the strains, thus facilitating the hydrogenation of silicene. In order to better display the effects strains on the hydrogenation of silicene, the energy barrier of a H_2 molecule dissociative adsorption on silicene under different strains is shown in Fig. 4. It is clearly shown that the both biaxial and armchair direction strains can reduce the energy barrier of the hydrogenation remarkably, but the energy barrier decreases the most efficiently under biaxial strain. Strain along zigzag direction also has effects on the barrier but is not very effective compared to the other two types of strains. When the strain is smaller than 8%, the two uniaxial strains have similar effects on the reduction of energy barrier. If further increasing the strains above 8%, the energy barrier of the system with the strain along armchair direction becomes much lower than the other uniaxial strain and reaches the same low barrier as the system under biaxial strain. In other words, applying biaxial strain and uniaxial strain along armchair direction to silicene can reduce the hydrogenation energy barrier more efficiently. When the strain increases to 12% or 13%, the energy barrier is reduced significantly from 1.71 eV to about 0.24 eV, which can facilitate hydrogenation of silicene significantly.

To better understand the effect of energy barrier reduction on the reaction reaction time, Eq. (2) is used to predict the reaction time τ at room temperature,[52]

$$\tau = \frac{1}{ve^{\left(\frac{-E_{bar}}{k_B T}\right)}} \quad (2)$$

where v is in order of 10^{12} Hz, k_B is the Boltzmann constant and T = 298.15 K. Without strain, $\tau = 8.06 \times 10^{16}$ s, while with 12% biaxial strain $\tau = 1.68 \times 10^{-8}$ s. As one can see, there is huge difference of the reaction time for the cases with and without strain.

The mechanism of the effect of tensile strain on energy barrier of silicene hydrogenation can be understood through analysing PDOS of the configuration at TS under different strains as shown in Fig. 5. The bands of *s* orbital of the two H atoms and the *p* orbital of the two corresponding Si atoms binding with the two H atoms at TS are provided. It is clear that the interaction of the Si-H interaction band of *s* orbital of H and *p* orbital of Si near Fermi level is significantly depressed under both biaxial strain and uniaxial tensile strain along armchair direction as the strains increase. It is known that the weaker interaction near Fermi level results in a lower energy barrier.[53] This could also explain strain along zigzag direction cannot reduce the barrier obviously because the interaction near Fermi level is depressed slightly. In addition, comparing the PDOSs under the biaxial and uniaxial along armchair strains, the interaction between Si and H atoms at TS for the case of biaxial strain drops more obviously. Therefore, the energy barrier decreases as the strains increasing and the effect of the biaxial strain is more obvious, which is consistent with the results in Figs. 3 and 4.

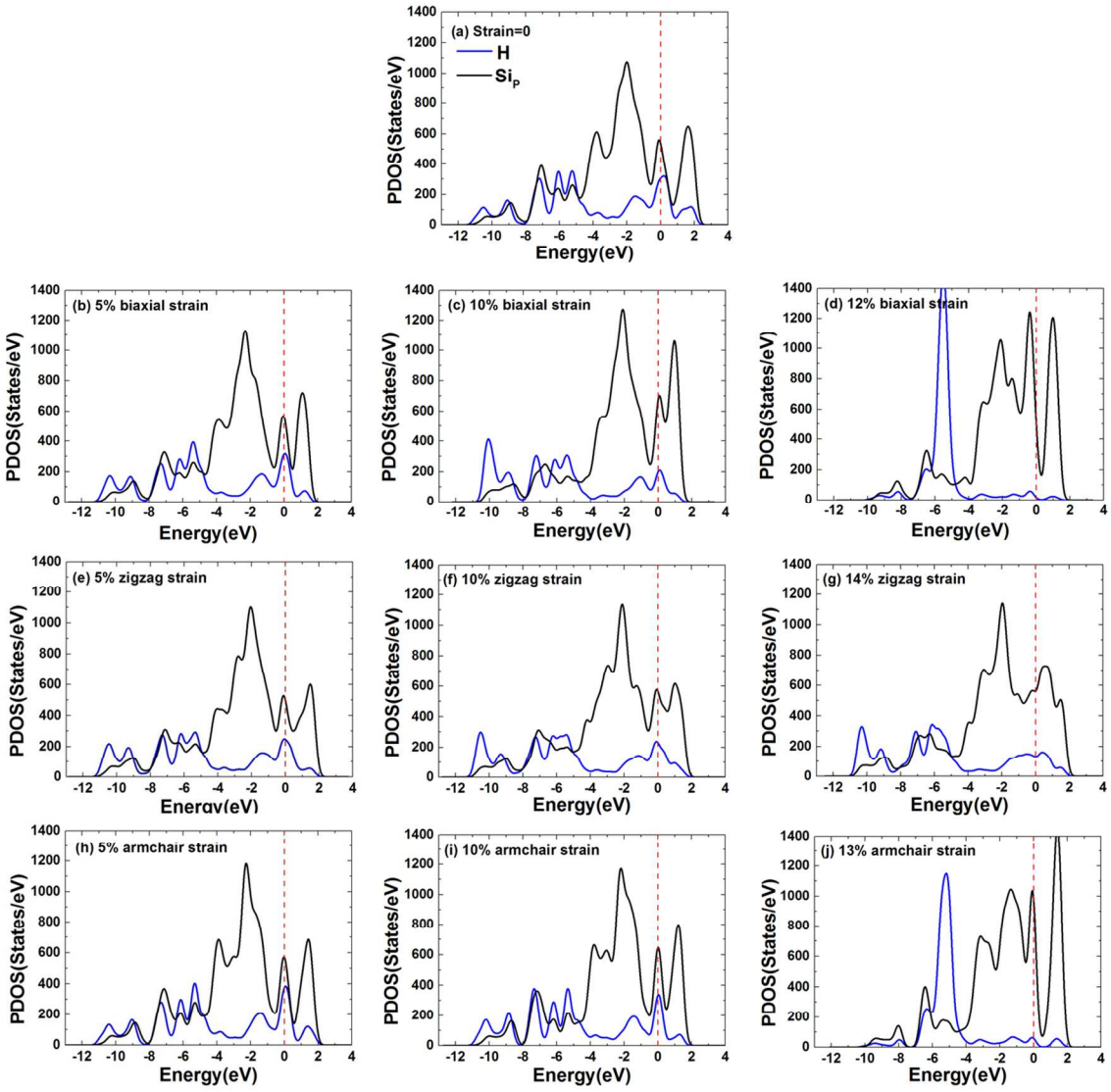

Fig. 5 The PDOS of the two H atoms and the two corresponding Si atoms at TS without strain (a), under increasing biaxial tensile strain [(b)-(d)], uniaxial tensile strain along zigzag direction [(e)-(g)] and along armchair direction [(h)-(j)]. The black curve is the PDOS of the two silicon atoms and the blue one indicates that of the two hydrogen atoms. The red dash line stands for the Fermi level.

The reduction of the energy barrier can be also understood through analysing the charge transfer between H atoms and silicene. When without strain, the atomic charges of one H atom and its corresponding Si atom in the reactant are -0.029 and 0.013 *e*, respectively. After dissociative adsorption, the charges are -0.053 and 0.054 *e*, respectively. It can be seen that the Si atoms are positive charged, while the H atoms are negatively charged. In other words, the electrons are transferred from Si to H atoms during hydrogenation. With all the three types of strains, the charges of H and Si atoms in the reactant are almost the same to the case of no strain, i.e. strain does not affect the interaction between H and Si much. This also agrees with the results in Tables 1, 2 and 3, where the adsorption energy does not change much under strains. However, after dissociative adsorption the atomic charges change remarkably. Under the maximum possible strains, the charge of the H atom decreases from -0.053 *e* to about -0.073 (biaxial), -0.064 *e* (armchair) and -0.057 *e* (zigzag) and the corresponding Si atom is positively charged with about 0.07 (biaxial), 0.065 *e* (armchair) and -0.057 *e* (zigzag) charges. Therefore, more electrons are transferred from the Si atoms to the H atoms under the biaxial strain, which would lead to easier binding of Si-H bonds during hydrogenation and thus contribute to the reduction of the energy barrier.

It is known that hydrogenation of silicene is an efficient way to open and tune the band gap of silicene for its potential applications in electronic devices.[16,19,38] To understand the effect of the strain and hydrogenation on the electronic properties, the band structure of silicene before and after hydrogenation with different biaxial strain is calculated as an example because the biaxial strain has the best effect to reduce the hydrogenation energy barrier. The results without strain and under 12% biaxial strains are shown in Fig. 6. Note that the band structure was calculated using CASTEP package using HSE06 hybrid functional due to more accurate band structure result. It can be seen from Fig. 6(a) that similar to graphene silicene is zero band gap material, the physical adsorption of H_2 does not change the pattern of the band structure near the Dirac point. While after hydrogen dissociative adsorption, the band gap opens

~0.34 eV as shown in Fig. 6(b). This means partial hydrogenation could also open the band gap of silicene due to the newly formatted Si-H bonds. This is also consistent with the reported result that the band gap of silicene depends on the ratio of hydrogenation, where half hydrogenated silicene turns out to be a semiconductor with a band gap about 0.84 eV [26] and fully hydrogenated silicene, named silicane, generates about 2 eV band gap.[37] Fig. 6(c) with 12% biaxial strain, the band gap of silicene at Dirac point does not open with π and π^* bands contacting at *K*-point under the biaxial strain, but the Fermi level shifts downwards. Thus, the biaxial strain cannot open the band gap of silicene due to the remaining symmetry. This result is also consistent with other report.[44] However, silicene transits from semimetal into metal due to the presence of bands at the Fermi level, which is also consistent with the reported result that this semimetal-metal transition occurs when the biaxial larger than 7%.[47] It can be understood because the buckled structure becomes flatter under big strain, which changes orientation of Si-Si bonds. For hydrogenated silicene, at Dirac point the band gap is still open under the stain, but the gap decreases to be ~0.12 eV. In addition, but the Fermi level shifts downwards, which also induces the semimetal-metal transition. Therefore, apply tensile strain is an effective method to tune the properties of silicone through hydrogenation. However, the stability of hydrogen on silicone should also been understood through investigating the hydrogen diffusion on silicene, similar to the reported works, where hydrogenation and diffusion on graphene[42,55] and on two-dimensional MoS_2[56] have been reported. Due to the complex of this work, such as considering the effects of strains, defects and external electric field on the hydrogen diffusion, we will show the corresponding results in another work.

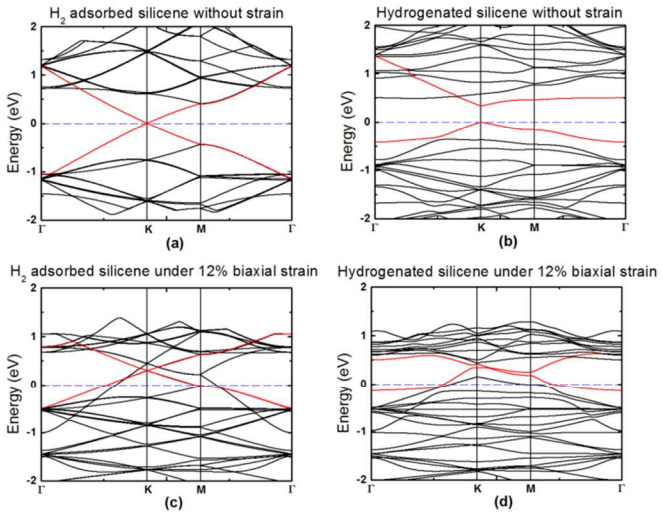

Fig. 6 Band structures of pure and hydrogenated silicene without strain [(a) and (b)] and under 12% biaxial strain [(c) and (d)]. The red lines are the bands near the Dirac point.

Conclusion

The dissociative adsorption of a H_2 molecule on silicene with different tensile strain is investigated by DFT calculations. It is found that the energy barrier of dissociative adsorption of a H_2 molecule on silicene can be reduced significantly by applying biaxial and uniaxial tensile strain along armchair direction, while the biaxial strain has the better effect to reduce the energy barrier. The energy barrier also decreases under the uniaxial strain along zigzag direction, but the effect is not so obviously. Under 12% biaxial strain, the energy barrier drops from 1.71 eV to about 0.24 eV, which can greatly reduce the reaction time from 8.06×10^{16} s to 1.68×10^{-8} s. Thus, the hydrogenation of silicene can be facilitated efficiently under the strains. Therefore, we propose an alternative method for hydrogenation of silicene, which is essential to tune its electronic properties for the application in electronic devices.

Acknowledgements

We acknowledge the financial supports from the Chancellor's Research Fellowship Program of the University of Technology, Sydney. This research was also supported by the National Computational Infrastructure (NCI) through the merit allocation scheme and used NCI resources and facilities in Canberra, Australia.

Notes and references

[a] School of Materials Science and Engineering, The University of New South Wales, Sydney, NSW 2052, Australia
[b] Centre for Clean Energy Technology, School of Chemistry and Forensic Science, University of Technology Sydney, PO Box 123, Broadway, Sydney, NSW 2007, Australia
[c] School of Physics and Optoelectronic Engineering, Nanjing University of Information Science and Technology, Nanjing 210044, China
[d] Nano Structural Materials Center, Nanjing University of Science and Technology, Nanjing 210094, Jiangsu, PR China
[e] Chongqing Key Lab for Advanced Materials & Clean Energies of Technologies, Institute for Clean Energy and Advanced Materials, Southwest University, 2 Tiansheng Rd, Beibei, Chongqing, China 400715

* Corresponding author. Email: Zhimin.ao@uts.edu.au

1 K. Takeda and K. Shiraishi, *Phys. Rev. B,* 1994, **50**, 14916.
2 G. G. Buzman-Verri and L. C. Lew Yan Voon, *Phys.Rev. B,* 2007, **76**, 075131.
3 B. Lalmi, H. Oughaddou, H. Enriquez, A. Kara, S. Vizzini, B. Ealet and B.Aufray, *Appl. Phys. Lett.,* 2010, **97**, 223109.
4 S. Q. Wang, *Phys. Chem. Chem. Phys.,* 2011, **13**, 11929.
5 C. C. Liu, W. X. Feng and Y. G. Yao, *Phys. Rev. Lett.,* 2011, **107**, 076802.
6 G. G. Buzman-Verri and L. C. Lew Yan Voon, *J. Phys.: Condens. Matter,* 2011, **23**, 145502.
7 X. Q. Wang, H. D. Li and J. T. Wang, *Phys. Chem. Chem. Phys.,* 2012, **14**, 3031.
8 C. W. Zhang and S. S. Yan, *J. Phys. Chem. C*, 2012, **116**, 4163.
9 M. Houssa, G. Pourtois, V. V. Afanasev and A. Stesmans, *Appl. Phys. Lett.*, 2010, **97**, 112106.
10 Y. C. Cheng, Z. Y. Zhu and U. Schwingenschlogl, *Europhys. Lett.*, 2011, **95**, 17005.
11 U. Rhlisberger, W. Andreoni and M. Parrinello, *Phys. Rev. Lett.,* 1994, **72**, 665.
12 H. Sahin, S. Cahangirov, M. Topsakal, E. Bekaroglu, E. Akturk, R. T. Senger and S. Ciraci, *Phys. Rev.B.*, 2009, **80**, 155453.
13 M. F. Cabrera, A. Munoz, W. Windl, A. A. Demkov, and O. F. Sankey, *Modell. Simul. Mater. Sci. Eng.,* 1999, **7**, 929.
14 L. Chen, C.-C. Liu, B. Feng, X. He, P. Cheng, Z. Ding, S. Meng, Y. Yao, and K. Wu, *Phys. Rev. Lett.*, 2012, **109**, 056804.
15 A. O. Hare, F. V. Kusmartsev and K. I. Kugel, *Nano Lett.*, 2012, **12**, 1045.
16 P. Zhang , X. D. Li , C. H. Hu, S. Q. Wu and Z. Z. Zhu, *Phys. Lett. A.,* 2012, **376**, 1230.
17 J. S. McEwen, P. Gaspard, F. Mittendorfer, T. Visart de Bocarmé and N. Kruse, *Chem. Phys. Lett.,* 2008, **452**, 133.
18 M. Houssa, E. Scalise, K. Sankaran, G. Pourtois, V. V. Afanasev and A. Stesmans, *Appl. Phys. Lett.,* 2011, **98**, 223107.
19 T. H. Osborn, A. A. Farajian, O. V. Pupysheva, R. S. Aga and L. C. Lew Yan Voon, *Chem. Phys. Lett.,* 2011, **511**, 101.
20 N. Gao, W. T. Zheng and Q. Jiang, *Phys. Chem. Chem. Phys.,* 2012, **14**, 257

21 H. Nakano, T. Mitsuoka, M. Harada, K. Horibuchi, H. Nozaki, N. Takahashi, T. Nonaka, Y. Seno and H. Nakamura, *Angew. Chem. Int. Ed.,* 2006, **118**, 6451.
22 C. Leandri, G. Le Lay, B. Aufray, C. Girardeaux, J. Avila, M. E. Davila, M. C. Asensio, C. Ottaviani and A. Cricenti, *Surf. Sci.,* 2005, **574**, L9.
23 B. Lalmi, H. Oughaddou, H. Enriquez, A. Kara, S. Vizzini, B. Ealet and B. Aufray, *Appl. Phys. Lett.,* 2010, **97**, 223109.
24 B. Aufray, A. Vizzini, S. Oughaddou, H. Leandri, C. Ealet and G. Le Lay, *Appl. Phys. Lett.,* 2010, **96**, 183102.
25 G. Le Lay, B. Aufray, C. Landri, H. Oughaddou, J. P. Biberian, P. De Padova, M. E. Dvila, B. Ealet and A. Kara, *Appl. Surf. Sci.,* 2009, **256**, 524.
26 D. C. Elias, R. R. Nair, T. M. G. Mohiuddin, S. V. Morozov, P, Blake, M. P. Halsall, A. C. Ferrari, D. W. Boukhvalov, M. I. Katsnelson, A. K. Geim and K. S. Novoselov, *Science,* 2009, **323**, 610.
27 S. Ryu, M. Y. Han, J. Maultzsch, T. F. Heinz, P. Kim, M. L. Steigerwald and L. E. Brus, *Nano Lett.,* 2008, **8**, 4597.
28 Z. Q. Luo, T. Yu, K. J. Kim, Z. H. Ni, Y. M. You, S. Lim, Z. X. Shen, S. Z. Wang and J. Y. Lin, *ACS Nano*, 2009, **3**, 1781.
29 Z. M. Ao, W. T. Zheng and Q. Jiang, *Nanotechnology,* 2008, **19**, 275710.
30 Z. M. Ao and F. M. Peeters, *Appl. Phys. Lett.,* 2010, **96**, 253106.
31 T. B. Martins, R. H. Miwa, A. J. R. da Silva and A. Fazzio, *Phys. Rev. Lett.,* 2007, **98**, 196803.
32 Z. M. Ao, S. Li and Q. Jiang, *Phys. Chem. Chem. Phys.,* 2009, **11**, 1683.
33 M. I. Katsnelson, K. S. Novoselov and A. K. Geim, *Nat. Phys.,* 2006, **2**, 620.
34 G. Gui, J. Li and J. Zhong, *Phys. Rev. B,* 2008, **78**, 075435.
35 L. Sun, Q. Li, H. Ren, H. Su, Q. W. Shi and J. Yang, *J. Chem. Phys.,* 2008, **129**, 074704.
36 F. B. Zheng and C. W. Zhang, *Nanoscale Res. Lett.*, 2012, **7**, 422.
37 L. C. Lew Yan Voon, E. Sandberg, R. S. Aga and A. A. Farajian, *Appl. Phys. Lett.,* 2010, **97**, 163114.
38 W. Wu, Z. M. Ao, T. Wang, C. Li and S. Li, *Phys. Chem. Chem. Phys.,* 2014, **16**, 16588.
39 A. Kara, H. Enriquez, A. P, Seitsonen, L.C. Lew Yan Voon, S. Vizzini, B. Aufray and H. Oughaddou, *Surf. Sci. Rep.,* 2012, **67**, 1.
40 P. R. Pereda and N. Takeuchi, *J. Chem. Phys.,* 2013, **138**, 194702.
41 N. Takeuchi and A. Selloni, *J. Phys. Chem. B,* 2005, **109**, 11967.
42 M. Yang, A. Nurbawono, C. Zhang, R. Wu, Y. Feng and Ariando, *AIP Adv.*, 2011, **1**, 032109.
43 H. Mckay, D. J. Wales, S. J. Jenkins, J. A. Verges and P. L. de Andres, *Phys. Rev., B,* 2010, **81**, 075425.
44 R. Qin, C. H. Wang, W. Zhu, and Y. Zhang *AIP Advances*, 2012, **2**, 022159.
45 C. Shang and Z. P. Liu, *J. Am. Chem. Soc.,* 2011, **133**, 9938.
46 G. Henkelman and H. Jonsson, *J. Chem. Phys.,* 2000, **113**, 9978.
47 G. Liu, M. S. Wu, C. Y. Ouyang and B. Xu, *EPL*, 2012, **99**, 17010.
48 T. Aizawa, R. Souda, S. Otani, Y. Ishizawa and C. Oshima, *Phys. Rev. Lett.,* 1990, **64**, 768.
49 B. Wang, J. Wu, X. Gu, H. Yin, Y. Wei, R. Yang and M. Dresselhaus, *Appl. Phys. Lett.* 2014, **104**, 081902.
50 C. Yang, Z. Yu, P. Lu, Y. Liu, H. Ye and T. Gao, *Comput. Mater. Sci.,* 2014, **95**, 420.
51 H. Zhao, *Phys. Lett. A,* 2012, **376**, 3546.
52 Q. G. Jiang, Z. M. Ao and Z. Wen, *Phys. Chem. Chem. Phys.,* 2014, **4**, 20290.
53 Z. M. Ao and F. M. Peeters, *Phys. Rev. B*, 2010, **81**, 205406.
54 Z. H. Ni, T. Yu, Y. H. Lu, Y. Y. Wang, Y. P. Feng and Z. X. Shen, *ACS Nano*, 2009, **3**, 483.
55 Z. M. Ao, A. D. Hernández-Nieves, F. M. Peeters and S. Li, *Phys. Chem. Chem. Phys.* 2012, **14**, 1463.
56 Y. Cai, Z. Bai, H. Pan, Y. P. Feng, B. I. Yakobson and Y. W. W. Zhang, *Nanoscale*, 2014, **6**. 1691.

Graphical and textual abstract

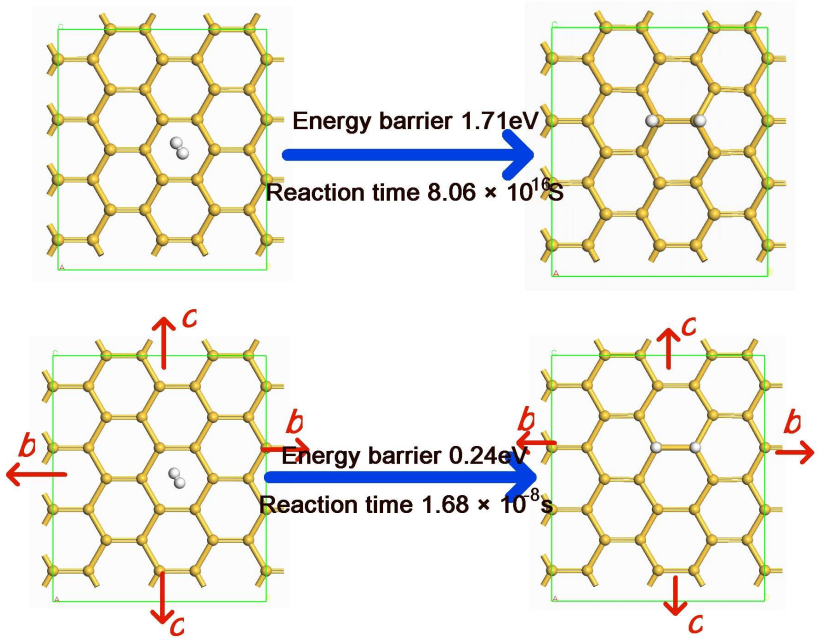

The energy barrier for hydrogenation of silicene decreases as the strains increase, and the barrier reduces from 1.71 to 0.24 eV when the strain reaches the critical value of 12%. In this way, the reaction time for the hydrogenation of silicene can accelerate significantly from 8.06 × 10^{16} to 1.68 × 10^{-8} s.